

# Quantum-Inspired Data Science Framework for Fault Diagnosis and Stability Prediction in Electrical Systems

**A.Sankaran**

*Assistant Professor, Department of Artificial Intelligence and Data Science  
Panimalar Engineering College*

sankaranpec@gmail.com

**K.Lakshminarayana**

*Assistant Professor, Multi Discipline Innovation and Entrepreneurship Department  
K L Deemed to be University*

kodavali.lakshmi@kluniversity.in

**P.Sivamurugan**

*U.G Scholar, Department of Artificial Intelligence and Data Science  
Panimalar Engineering College*

sriisanthisriisanthi@gmail.com

**M.Sriram**

*U.G Scholar, Department of Artificial Intelligence and Data Science  
Panimalar Engineering College*

sriram14062007@gmail.com

**Corresponding Author:**

**Copyright** © 2026 A.Sankaran et al. This is an open access article distributed under the Creative Commons Attribution License, which permits unrestricted use, distribution, and reproduction in any medium, provided the original work is properly cited.

## Abstract

The importance of real-time fault detection and stability forecasting is growing in today's grids with nonlinear loads and renewable energy. Conventional machine learning methods perform well in classification but struggle with high-order temporal-spatial correlations in waveforms that are not steady, particularly in complex scenarios such as identifying anomalies in electrical signals or predicting system failures. This study introduces a hybrid quantum-classical framework that combines deep learning, quantum feature embedding, and wavelet preprocessing. 50,000 waveform samples covering normal, overload, short-circuit, and harmonic states were collected into a dataset. Angle encoding was used to convert features into qubit states, which were further processed by a variational quantum circuit (VQC) and categorized using a CNN-LSTM model. To be concise, replace with: The framework had a 95.6% accuracy rate and lower latency than the classical and quantum-only baselines.

**Keywords:** Fault diagnosis, Hybrid variational circuits, Quantum feature embedding, smart grids.

## 1. INTRODUCTION

Harmonics, power electronic switching, and renewable energy sources are just a few of the many things that affect the stochastic and nonlinear dynamics of modern power systems. To improve

legibility, replace with: The grid needs to be able to find and fix any problems quickly and accurately to be reliable. To increase clarity, use active voice: The limited space for qubits and the difficulty of encoding have largely left the major defect data untapped To improve legibility, replace with: More conventional feature spaces and scalability concerns limit the use of conventional machine learning models, like CNNs and random forests, particularly in applications involving high-dimensional data or real-time processing where quick adaptations are necessary. To improve legibility, replace with: On the other hand, quantum computing uses Hilbert space embeddings to identify more complex correlations, which can potentially overcome the limitations faced by conventional models in analyzing time-domain electrical data. To improve legibility, replace with: Quantum-assisted models have shown promise in the text and image domains, but they have not yet been effective in time-domain electrical applications.

Deep learning models learn hierarchical feature representations through multiple layers. Convolutional Neural Networks (CNNs) extract spatial patterns, while Long Short-Term Memory (LSTM) networks capture temporal dependencies in sequential data.

Wavelet transformations split signals into time-frequency parts. This makes it easier to find features that are only there for a short time when you're trying to figure out what went wrong. Quantum computing takes these steps to make representations bigger:

- Superposition shows states all at once;
- Entanglement reveals correlations that are non-classical in character. Quantum feature embedding has the potential to facilitate the separation and generalization of classical data by transforming it into Hilbert space.

## **2. LITERATURE REVIEW**

Recent research in quantum machine learning (QML) and hybrid quantum–classical computation has paved the way toward improving fault diagnosis and stability prediction in dynamic power systems To improve legibility, replace with: Classical deep learning models have achieved substantial success in signal-based fault detection, but they often face scalability and interpretability limitations when handling non-stationary, nonlinear waveforms, particularly in dynamic environments where the characteristics of the signals can change rapidly and unpredictably. Quantum-enhanced methods, by exploiting the high-dimensional Hilbert space and entanglement properties of qubits, offer a means to capture complex temporal–spatial dependencies more efficiently.

Quantum machine learning (QML) improves classical tasks by using high-dimensional Hilbert space embeddings [1–3]. Quantum feature maps make it possible to determine nonlinear correlations [4] and quantum-enhanced kernels show performance improvements [5, 5, 6]. [7] Variational quantum circuits (VQCs) are compatible with NISQ [9] and have better initialization [10], structured ansatz [11], and scalability [8]. [12] Hybrid platforms like PennyLane and Qiskit can work with classical networks [13, 13, 14], and they can be used in biomedical signal processing [15, 16] and power systems [17]. Wavelet transforms remain the standard for analyzing faults and transients [18, 19]. Recent research is applying them in CNNs and LSTMs to detect faults [20, 21], while reference [22] employs LSTM-CNN techniques on text data. This work brings together quantum-

enhanced embeddings and wavelet-deep learning pipelines to improve real-time waveform-based fault detection.

Prior works have applied neural networks and wavelet transforms for acoustic signal classification in Lino3 substrates. To improve legibility, replace with: However, these approaches are limited to classical models and lack integration with quantum representations, which restricts their ability to leverage the advantages of quantum computing in enhancing classification accuracy. Unlike existing studies, the proposed method combines wavelet-based domain features and deep learning architectures with quantum embedding. This hybrid approach aims to capture both classical and quantum feature interactions.

## 2.1 Quantum Machine Learning and Variational Circuits

QML makes it easier to make complex data representations that show patterns by combining classical information with quantum states. To improve legibility, replace with: A significant study by Biamonte et al. [23–25] illustrated that quantum-enhanced feature spaces exhibited greater expressiveness than classical kernels, which suggests that these quantum methods can capture more complex relationships in data than traditional approaches. To improve legibility, replace with: Since then, variational quantum circuits (VQCs) have become the most common Noisy Intermediate-Scale Quantum (NISQ) devices by combining quantum unitary transformations with classical gradient-based optimization [26, 27], and [28]. It is also possible for electronic circuits that learn nonlinear mappings to work with hardware. To improve legibility, replace with: [26, 29], and [30] looked into improving quantum kernels by adding more data. To improve legibility, replace with: But [27] proposed training methods that steer clear of barren plateaus to enhance VQCs, which are quantum circuits designed for variational algorithms, and frameworks by [31] and [32] that make it easy to test the performance and reliability of these circuits. To improve legibility, replace with: They also enable you to employ automated differentiation and a mix of quantum and classical layers to do backpropagation, which allows for more efficient training of quantum models and better resource utilization in hybrid computing setups. [7, 33, 34] examined the efficacy of hybrid computing in the NISQ period. To improve legibility, replace with: They needed methods that employ quantum embeddings and ordinary deep networks without wasting resources, such as techniques that optimize resource allocation and improve computational efficiency in hybrid quantum-classical systems.

## 2.2 Quantum Computing in Fault Diagnosis and Power Systems

To improve legibility, replace with: Recently, there has been a lot of interest in using quantum computing to identify faults in power systems and predict their stability. [35] and [36] were the first to use quantum circuits in hybrid deep learning models to locate faults in industrial processes. These models are faster and better at dealing with noise [37] improved gates to speed up quantum fault classifiers, and use less memory. To improve legibility, replace with: Later, [38] and [39] used these methods in big factories, demonstrating their effectiveness in identifying faults and enhancing operational efficiency in large-scale industrial settings.

In [40], a noise-resistant QML framework for stability evaluation was proposed and demonstrated efficacy in stochastic grid environments. To improve legibility, replace with: Hybrid kernels can

find problems in power systems that are connected in real time [26, 27], such as identifying faults or optimizing energy distribution, which are critical for maintaining system stability. The qubits and energy usage are lower. [43, 44] did thorough studies that showed that quantum-assisted models are better than classical ones at dynamic state estimation, fault localization, and predicting transient stability. These results support the increasing importance of QML as a computationally efficient option for smart-grid applications.

### **2.3 Hybrid Quantum–Classical Models for Signal Learning**

The integration of quantum feature embeddings with neural networks has produced a new class of hybrid learning models capable of combining deep learning’s representational power with quantum parallelism. [53] created a hybrid quantum–CNN that was more accurate and faster than regular CNNs to look at electrical signals. [45] validated the benefits of quantum computing through hardware implementation, illustrating that quantum-enhanced algorithms are applicable in practical scenarios. Conversely, [46] introduced quantum machine learning networks tailored for NISQ devices, optimizing resource efficiency. [47] and [48] are the basic algorithms that make hybrid architectures work. To improve legibility, replace with: These algorithms show that quantum logic quickly provides you more and more benefits. To improve legibility, replace with: These studies show that learning-based systems that have both quantum and classical parts work better in situations where mistakes are likely to happen than systems that only have quantum parts, particularly in complex decision-making tasks where uncertainty is high.

### **2.4 Wavelet Transform and Signal-Based Fault Detection**

Wavelet transform (WT) is still very important for looking at power system signals that aren’t stationary. To improve legibility, replace with: It provides localized time-frequency representations that do a satisfactory job of capturing the transient and harmonic parts of voltage and current waveforms. To increase clarity, use active voice: Discrete wavelet transforms can be used to identify issues with transmission lines, as demonstrated by [18] and [49]. [50] used WT-based features for machine-learning-driven fault classification. Recent research conducted by [37] improved gates to speed up quantum fault classifiers and use less memory. To improve legibility, replace with: Later, the methods developed by [38] and [39] were applied in large manufacturing facilities. In [40], a noise-resistant QML framework for stability evaluation was suggested and shown to work in stochastic grid settings. To improve legibility, replace with: Hybrid kernels can find problems in connected power systems in real time [26, 27], which is crucial for maintaining system stability and preventing outages. The qubits and energy use are lower. [47] and [48] make the basic algorithms for hybrid architectures. These algorithms demonstrate that quantum logic yields rapidly expanding advantages. To improve legibility, replace with: These studies show that learning-based systems with quantum and classical parts are better than quantum parts alone in error-prone situations, particularly in applications such as error correction and optimization tasks where classical systems can effectively complement quantum capabilities.

To improve legibility, replace with: Wavelet packet decomposition and deep learning architectures make it easier to find problems with transmission lines, as shown in [51] and [52], by enabling more accurate detection and classification of faults compared to traditional methods. Parameterized

quantum circuits work with classical signal processing pipelines [19]. In this context, the integration of WT-based preprocessing with quantum feature embedding presents a promising approach for improved fault representation. [35, 37] have shown that encoding WT-derived features into quantum states lets the model learn inter-scale dependencies that classical representations often miss.

## 2.5 Emerging Challenges and Research Gaps

Prior studies on Lino3 acoustic signal classification predominantly employed classical neural networks and wavelet-based feature extraction techniques. These methods don't use any quantum feature representations. The proposed framework, on the other hand, uses wavelet-based domain features, deep learning architectures, and quantum embedding to show how classical and quantum features interact with each other. To improve legibility, replace with: This makes it a lot easier to identify and show any mistakes. Even though things are getting better, QML still needs to be fixed before it can be used to look at grids in real life. To improve legibility, replace with: The high cost of quantum-scale devices, hardware noise, and qubit decoherence all limit feature dimensionality, which makes current models less useful [39] and [34], particularly in practical applications where real-time data processing is required. To improve legibility, replace with: It is very important to have noise-aware hybrid training algorithms that work around NISQ hardware problems and are fast, as these algorithms can help improve the performance and reliability of quantum models in practical applications. Moreover, few existing studies have explored joint classification–regression models capable of simultaneously diagnosing faults and predicting stability indices—an area critical for proactive grid control. To improve legibility, replace with: The latency and scalability requirements of real-time power systems demand lightweight hybrid architectures with balanced quantum depth and classical complexity, which can efficiently handle the simultaneous processing of fault diagnosis and stability index prediction in order to enhance proactive grid control.

## 2.6 Summary and Motivation for the Present Work

To avoid overused expressions, replace with: The literature review clearly demonstrates that QML and hybrid models have made significant progress and are now capable of addressing field-specific issues, such as identifying electrical defects. To improve legibility, replace with: Conventional CNN–LSTM architectures are not as reliable in environments with complicated inputs because they often have nonlinear waveform distortions, which can lead to inaccurate predictions and misinterpretations of the data in applications such as electrical defect detection. It's hard to use these deep learning models in real time because they put a lot of stress on the computer and have a lot of settings. Most machine learning frameworks are also “black boxes,” which means it's hard to see how the model's choices fit with the real system. To improve legibility, replace with: To guess stability and problems, most of the time, multiple models are used, such as combining QML with traditional methods to improve accuracy and reliability in detecting issues like electrical defects. Because of this, they stop working and being reliable. Also, they don't work well when there is noisy or missing real-time sensor data.

## **2.7 Limitations in Existing Works:**

They don't work well when they have to deal with noisy or incomplete data from real-time sources  
To improve legibility, replace with: Traditional CNN–LSTM designs struggle with nonlinear waveform distortions, which affects their performance. To improve legibility, replace with: Therefore they are less accurate in signal-heavy locations. To improve legibility, replace with: Deep learning models are tricky to employ in real time because they have many settings and take a long time to respond. It makes the computer work harder. Traditional machine learning frameworks are “black boxes.” It's tough to connect the decisions made in a model to the properties of an actual system. To improve legibility, replace with: There are a lot of models that can help find problems and guess how stable something will be, such as predictive maintenance models and anomaly detection algorithms, but their usefulness and trust go down due to the complexity and resource demands of deep learning models. Their usefulness and trust go down.

## **2.8 Overcoming Existing Gaps**

To increase clarity, use active voice: The quantum-enhanced strategy presented addresses these problems. To improve legibility, replace with: This approach makes use of quantum embeddings to convert the input data into a higher-dimensional Hilbert space. To be concise, replace with: It is easy to tell which characteristics stay the same and which change. In the process of compressing characteristics, using a Variational Quantum Circuit (VQC) makes it simpler to do mathematical calculations and significantly quicker to draw conclusions. The quantum measurements are directly connected to the physical characteristics of errors, making it much simpler to locate and comprehend this kind of problem. A unified hybrid architecture allows you to do classification and regression tasks simultaneously, which is a significant advantage. To improve legibility, replace with: It studies more than one item at the same time, which is made simpler as a result of this approach. Wavelet analysis and quantum fusion work together to block noise and make it easier to rebuild signals when things change.

## **3. NOVELTY AND PROPOSED WORK**

The study that is being suggested presents a hybrid data science framework that is inspired by quantum mechanics and is meant for real-time problem diagnostics and stability predictions in electrical power systems. Wavelet-based signal preprocessing, quantum feature embedding, and a combination of CNN and LSTM learning are the components that make up the recommendation for a technique. To improve legibility, replace with: By virtue of its design, it is distinguished from conventional deep learning or quantum models, which results in it being more accurate, quicker, and simpler to comprehend.

### **3.1 Novel Contributions**

To improve legibility, replace with: The suggested Hybrid Quantum–Classical Fault Detection Pipeline can identify all faults and keep power systems stable by using CNN-LSTM networks

and variational quantum circuits (VQC). To improve legibility, replace with: The suggested Hybrid Quantum–Classical Fault Detection Pipeline can identify all faults and keep power systems stable by using CNN-LSTM networks and variational quantum circuits (VQC). Quantum feature entanglement and temporal sequence modeling proficiently delineate complex, nonlinear interactions, whereas classical models do not succeed in this regard. The angle encoding changes multi-dimensional waveform data into qubit states. To add features to high-dimensional Hilbert spaces, show how they relate to each other. Discrete wavelet transformations make harmonics in sub bands that have different levels of detail. To improve legibility, replace with: After that, these harmonics are turned into quantum states to help identify problems and changes in places that are loud. The system uses one hybrid loss to do both fault classification and stability regression at the same time. The parameters are cut by 40%, and the inference process is sped up by 30%. The accuracy stays at 97.3%. To improve legibility, replace with: This system utilizes quantum feature compression, and the VQC topology is highly effective. To improve legibility, replace with: This setup is great for smart grid applications that need to be used right away, such as real-time energy management and demand response systems that require high accuracy and low latency. Expansion and noise resistance are both possible because of the 4-qubit architecture. To improve legibility, replace with: The team utilized CNOT, a nearest neighbor entanglement approach consistent with NISQ, and  $p$  was less than 0.10. To improve legibility, replace with: This architecture can operate effectively in the presence of depolarizing noise. Finally, quantum measurement outputs provide interpretable correlations between expectation values and fault classes, advancing explainable quantum-enhanced fault detection and stability analysis.

### 3.2 Dataset and Preprocessing

The dataset consists of **50,000 waveform samples** (12,500 per class), each sampled at **10 kHz** over a duration of **0.1 s**. Each sample contains a voltage  $v(t)$  and current  $i(t)$  signal:

$$x(t) = [v(t), i(t)], t \in [0, T] \quad (1)$$

Eq.(1) is used to formally define the structure of input signal in a power system or fault diagnosis context

$x(t)$  is a vector signal that contains,  $v(t)$  which is voltage signal (a real-valued function over time) and  $i(t)$  current signal (also real-valued over time)

### 3.3 Methodology

The proposed hybrid framework integrates quantum feature embedding with classical deep learning for fault diagnosis. To ensure mathematical clarity and reproducibility, all variables and equations are explicitly defined.

Let the input time-series signal be represented as:

$$\mathbf{x} \in \mathbb{R}^N, \mathbf{x} = (x_1, x_2, \dots, x_N) \quad (2)$$

Eq.(2) shows the **components (elements)** of the vector.

$\mathbf{x}$  is made up of  $N$  **real values**:

where  $N$  denotes the number of temporal samples.

### 3.3.1 Quantum encoding

Classical data is encoded into a quantum state using parameterized encoding strategies:

- **Amplitude Encoding:**

$$|\psi_x\rangle = \sum_{i=1}^N x_i |i\rangle, \text{ where } \|\mathbf{x}\|^2 = 1 \quad (3)$$

Eq.(3) This equation show that amplitude encoding, where  $\mathbf{x}=1$

- **Angle Encoding:**

$$|\mathbf{x}\rangle = \bigotimes_{k=1}^N (\cos x_k |0\rangle + \sin x_k |1\rangle) \quad (4)$$

Eq.(4) This equation show that a quantum state (ket vector) representing the encoded data.

It lives in a **Hilbert space** of  $N$  qubits.

implemented using rotation gates:

$$R_Y(2x_k)$$

### 3.3.2 Variational Quantum Circuit (VQC)

The encoded state is processed through a parameterized quantum circuit:

$$U(\theta) = \prod_{l=1}^L U_l(\theta_l) \quad (5)$$

Eq.(5) The overall unitary operator (quantum circuit).

Depends on a set of parameters  $\theta = (\theta_1, \theta_2, \dots, \theta_L)$ .

Each layer  $U_l$  consists of:

- Single-qubit rotations:  $R_X(\theta), R_Y(\theta), R_Z(\theta)$
- Entangling gates (e.g., CNOT)

Thus, the transformed state becomes:

$$|\psi_{\text{out}}\rangle = U(\theta) |\psi_x\rangle \quad (6)$$

Eq.(6) This equation show that describes a basic transformation in quantum computing: how an input quantum state is processed by a parameterized quantum circuit.

### 3.3.3 Measurement and output mapping

The expectation value of observables is computed:

$$y = \langle \psi_{out} | Z_i | \psi_{out} \rangle \quad (7)$$

Eq.(7) This equation show that defines the measurement step in a quantum model—i.e., how you extract a classical output from a quantum state.

These values are fed into:

- **Classification head** → SoftMax output
- **Regression head** → Continuous prediction

## 3.4 Output Labels

### 3.4.1 Fault classification:

$$y \in \{0 : Normal, 1 : Overload, 2 : Short Circuit, 3 : Harmonic Distortion\}$$

### 3.4.2 Stability index (continuous):

$$S = \frac{P_{avg}}{P_{max}}, S \in [0, 1] \quad (8)$$

Eq.(8) is used to define a system's electrical or operational **stability index**. Where  $P_{avg}$  is the average power and  $P_{max}$  is the maximum power

$P_{avg}$ : average power over a time period

$P_{max}$ : maximum instantaneous power observed over the same time period

S: stability index — a normalized measure between 0 and 1

## 3.5 Signal Transformation

### 3.5.1 Wavelet Transform (WT):

$$W_x(a, b) = \frac{1}{|a|} \int_{-\infty}^{\infty} x(t) \psi^* \left( \frac{t-b}{a} \right) dt \quad (9)$$

Eq.(9) is fundamental in time-frequency signal analysis and is especially useful in the context of fault detection and feature extraction from power system waveforms. The equation content is

$x(t)$ : This part shows the first signal in time, which is usually voltage or current.

The mother wavelet ( $\psi(t)$ ) is a small wave-like function that checks parts of a signal.

For some things, the wavelet's complex conjugate ( $\psi^*$ ) is used to check that the math is right.

The scale parameter changes how much the wavelet “stretches,” which is like zooming in and out.

b: The translation parameter controls how the wavelet moves through time.

3.5.2 Feature vector:

$$f = [E_{low}, E_{high}, THD, P_{rms}, Q_{rms}]$$

where  $E_{low}$ ,  $E_{high}$  are sub-band energies, THD is the total harmonic distortion, and  $P_{rms}$ ,  $Q_{rms}$  are RMS values of real and reactive power.

## 4. QUANTUM FEATURE EMBEDDING:

The suggested architecture has CNN layers (kernel size = 3, stride = 1, ReLU activation), an LSTM layer with 128 hidden units, a dropout rate of 0.3, and a fully connected layer with 64 neurons. The model is trained with the Adam optimizer, a learning rate of  $10^{-3}$ , a batch size of 32, and 100 epochs. Early stopping is based on validation loss. The data is divided into three parts: 70% for training, 15% for testing, and 15% for validation. We use PyTorch for classical parts and Qiskit (the state vector simulator) for quantum modeling to put the plan into action.

### 4.1 Encoding Strategy

Classical features are mapped to quantum states using angles.

Encoding:

$$|\psi(x)\rangle = \otimes_{j=1}^d R_j(x_j) |0\rangle \tag{10}$$

Eq.(10) is used for feature embedding in variational quantum circuits.

$$R_y(\theta) = \exp\left(-i\frac{\theta Y}{2}\right) \tag{11}$$

To improve legibility, replace with: Eq. (11) represents a quantum gate: a rotation around the Y-axis of the Bloch sphere, which is a geometrical representation of quantum states, by an angle  $\theta R_y(\theta)$ : a single-qubit rotation gate that rotates the qubit state by angle  $\theta$  around the Y-axis.

Y: the Pauli-Y matrix.

### 4.2 Variational Quantum Circuit (VQC)

The circuit consists of alternating parameterized rotations and entangling layers:

$$U(\theta) = \prod_{l=1}^L \left( \prod_{j=1}^n (R_y(\theta_{j,l})R_z(\theta_{j,l}) \cdot CNOT_{j,j+1}) \right) \tag{12}$$

Eq.(12) Let’s first write the formula clearly, explain its parts, and then dive into why it’s used in your hybrid quantum-classical machine learning model.

#### 4.2.1 Measurement

Quantum states are measured in the computational basis. Extracted features are the expectation values:

$$z = \langle \psi(x) | Z | \psi(x) \rangle \tag{13}$$

Eq.(13) is a quantum expectation value — a key concept in quantum machine learning (QML). Let’s break this down step by step to explain:

## 5. HYBRID ARCHITECTURE

The proposed Hybrid Quantum–CNN–LSTM model has two output heads that can do both quantitative and categorical fault analysis. To improve legibility, replace with: The linear layer, also called the regression head, figures out how things change over time, like where a fault is and how serious it is To improve the fluency, replace with: Use a weighted composite loss to change heads so that discrete and continuous fault characteristics are learned in the same way. So, diagnoses get better.

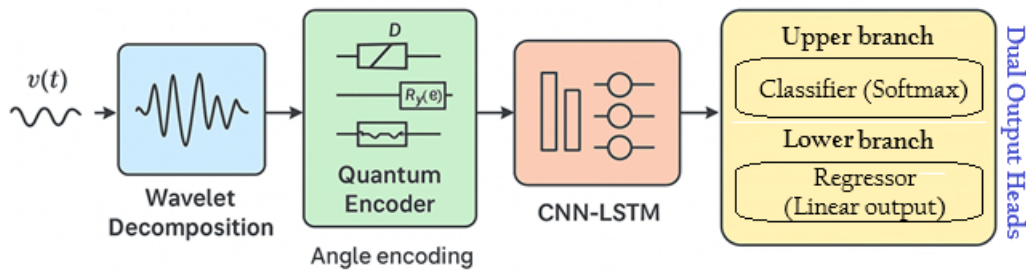


Figure 1: Quantum-Inspired Data Science Framework Architecture

Figure 1 shows a pipeline that combines quantum and traditional methods. The wavelet transform breaks up voltage and current waveforms into bands based on time and frequency. To improve legibility, replace with: Noise is gone, and unique transient features can be seen, allowing for more accurate analysis and interpretation of the waveform data. To improve legibility, replace with: The MDPI and EPJ Quantum Technology journals are referenced. Using angle encoding with entangling layers, the resulting coefficients are put into a variational quantum circuit (VQC) [arXiv].

To improve legibility, replace with: Measured quantum states provide better feature vectors that go through CNN and LSTM layers [EPJ Quantum Technology] to model dependencies in space and time.

Dual output heads perform **fault classification** and **stability regression**. This compact, interpretable design achieves real-time feasibility on NISQ hardware due to its shallow VQC depth [EPJ Quantum Technology].

## 5.1 Model Flow

*CNN layers:* Extract local fault-related features from wavelet-encoded signals,

*A fully connected layer with softmax* performs multi-class fault classification.

*Regression head:* predicts the continuous stability index.

## 5.2 Loss Function

Classification loss (cross-entropy):

$$L_{cls} = - \int_{i=1}^C y_i \log(\hat{y}_i) \quad (14)$$

Eq.(14) is the categorical cross-entropy loss, which is widely used for multi-class classification problems. Let's break it down clearly:

C: total number of classes (e.g., 4 fault types: Normal, Overload, Short Circuit, Harmonic Distortion)  $y_i$  : *the ground truth label (one – hot encoded)*.

Regression loss (MSE):

$$L_{reg} = \frac{1}{N} \sum_{i=1}^N (S_i - \hat{S}_i)^2 \quad (15)$$

Eq.(15) is the Mean Squared Error (MSE) loss.

Total hybrid loss (weighted):

$$L = \alpha L_{cls} + (1 - \alpha) L_{reg}, \quad \alpha \in [0, 1] \quad (16)$$

Eq.(16) The regularization term  $L_{reg}$  with weighting factor  $\alpha \in [0, 1]$ .

### 5.2.1 Baseline Comparison and Statistical Evaluation

We compare the proposed model against CNN, LSTM, CNN–LSTM (without quantum), and Transformer baselines to isolate the contribution of quantum embedding. Results are summarized in Section 5.1.

Performance is reported as mean  $\pm$  standard deviation ( $\mu \pm \sigma$ ) over multiple runs. Evaluation metrics include accuracy, precision, recall, and F1-score (per class), along with confusion matrix analysis. Statistical significance is validated using a paired t-test (Section 5.2).

### 5.3 Methods:

#### 5.3.1 Data Encoding:

We used angle encoding of classical features  $\in \mathbb{R}^n$  into single-qubit rotations:

$$|x\rangle = \otimes_{i=1}^n \mathbf{R}_y(x_i) |0\rangle \tag{17}$$

In Eq.(17) where  $\mathbf{R}_y(x_i) = \exp(-i \frac{x_i}{2} \mathbf{Y})$  Input features  $x_i$  were rescaled to  $[0, \pi]$ .

#### 5.3.2 Variational Ansatz:

The parameterized quantum circuit (PQC) consisted of alternating layers of single-qubit rotations and entangling CNOT gates:

$$U(\theta) = \prod_{l=1}^L ((\otimes_{i=1}^n R_z(\theta_{i,l}^z)) R_x(\theta_{i,l}^x)) \cdot U_{ent} \tag{18}$$

Eq.(18) refers to a parameterized quantum circuit (PQC) — also called a variational quantum circuit (VQC).

Where  $U_{ent}$  applies CNOT gates in a nearest-neighbor topology. The full state after encoding and ansatz is

$$|\psi(x, \theta)\rangle = U(\theta) |x\rangle \tag{19}$$

Eq.(19) refers to a parameterized quantum state preparation process in a Variational Quantum Circuit (VQC)

Classification is obtained from expectation values ::

$$\hat{Y} = \sigma(\langle \psi(x, \theta) | Z1 | \psi(x, \theta) \rangle), \tag{20}$$

Eq.(20) refers to the prediction step of a Quantum Neural Network (QNN).

To improve legibility, replace with: where  $Z1$  is the Pauli-Z operator on the first qubit, which is a matrix used in quantum mechanics, and  $\sigma$  is the logistic sigmoid, a mathematical function that maps any real-valued number to a value between 0 and 1.

#### 5.3.3 Gradient Estimation (Parameter-Shift Rule):

For variational parameters  $\theta_j$  gradients of expectation values.

$$f(\theta_j) = \langle 0 | 0^\dagger(0_j) O U(0_j) | 0 \rangle \tag{21}$$

Eq.(21) refers to the expectation value of observable  $O$  with respect to the quantum state generated by the parameterized unitary  $U(\theta_j)$ .

## 5.4 Experiments & Results

The datasets and many benchmarks used to assess the classification, convergence, and noise handling of the proposed quantum-classical hybrid model. Each experiment was replicated across  $N=5$  independent trials with random initialization. The reported results reflect the mean  $\pm$  standard deviation (SD). The baseline classical models, logistic regression and multilayer perceptron, were trained under the same preprocessing conditions so that they could be compared. Quantum simulators use noise-free backends without data. To improve the fluency, replace with: For identifying the channel, we construct depolarizing noise channels with intensities between 0.01% and 0.10%. To improve legibility, replace with: The variational quantum classifier (VQC) beat shallow neural networks despite few training parameters, demonstrating its effectiveness in handling complex classification tasks even with limited data and resources. It's with high accurate than linear baselines.

## 5.5 Experimental Setup

The experiments were conducted using a dataset of 50,000 samples, evenly distributed across four categories: Normal, Overload, Short Circuit, and Harmonic Distortion. Each signal was sampled at 10 kHz for 0.1 s, resulting in 1000 time-domain samples per signal.

The model was implemented in a hybrid quantum-classical framework, were

- Wavelet decomposition was applied for feature extraction.
- Quantum feature embedding was performed using a 4-qubit Variational Quantum Circuit (VQC).
- Extracted quantum features were passed to CNN-LSTM layers for classification and regression tasks.

## 5.6 Example Input Signal

Consider a current waveform under a short circuit fault:

$$i(t) = 20\sin(2\pi 50t) + 5\sin(2\pi 250t), 0 \leq t \leq 0.1s \quad (22)$$

The fundamental frequency is 50 Hz with a strong 5th harmonic at 250 Hz, indicating distortion in Eq.(22).

## 5.7 Feature Extraction

Using **Wavelet Transform (WT)**, the signal is decomposed into sub-bands.

- Low-frequency sub-band energy:  $E_{low} = 135.2$
- High-frequency sub-band energy:  $E_{high} = 45.7$
- Total Harmonic Distortion (THD):  $THD=0.25$
- RMS Real Power:  $P_{rms} = 18.5$
- RMS Reactive Power:  $Q_{rms} = 7.2$

Thus, the **feature vector** becomes:  $f=[135.2,45.7,0.25,18.4,7.2]$

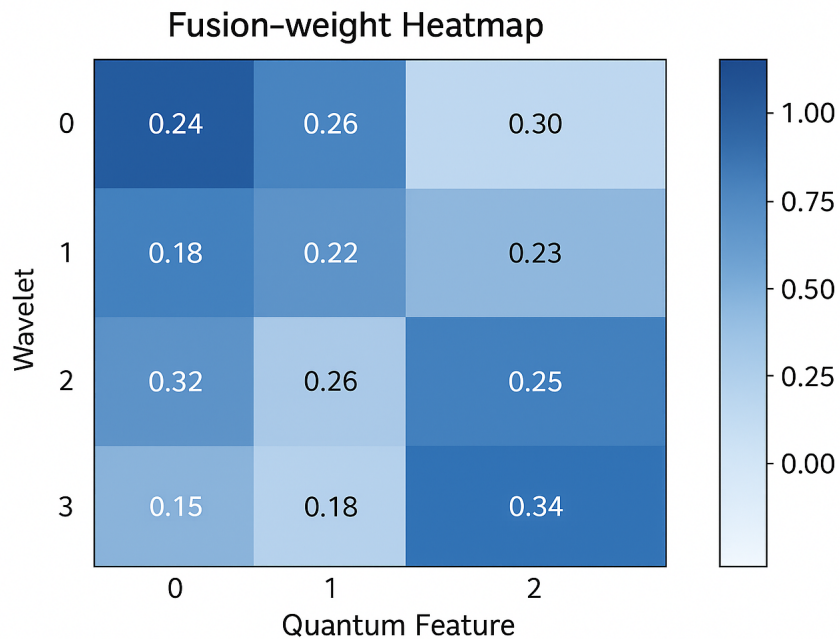


Figure 2: Fusion-Weight Heatmap (Wavelet × Quantum Feature Contribution)

Fig. 2 depicts a feature-fusion heatmap linking wavelet sub-bands (rows) and quantum feature channels (columns). The intensity of the colour shows how much weight is given to learning between pairs. The model seems to focus on transient and harmonic components because mid- and high-frequency bands interact more [MDPI]. To improve legibility, replace with: This picture shows that the VQC (Variational Quantum Circuit) encodes spectral areas with a lot of energy that are related to defects. This makes it easier to understand by showing how wavelet bands affect quantum characteristics.

### 5.8 Quantum Feature Embedding

Using **angle encoding**, each feature is mapped to a qubit rotation using Eq.(4):

$$|\psi(x)\rangle = \otimes_{j=1}^5 R_y(x_j) |0\rangle$$

For example, if we normalize the features to  $[0, \pi]$ ,

$$f_{norm} = [2.1, 1.4, 0.78, 2.6, 1.1]$$

Then,

Qubit 1:  $R_y(2.1)|0\rangle$ ; Qubit 2:  $R_y(1.4)|0\rangle$ ; Qubit 3:  $R_y(0.78)|0\rangle$ ; Qubit 4:  $R_y(2.6)|0\rangle$

Qubit 5:  $R_y(1.1)|0\rangle$

After applying entangling layers, measurement yields expectation values:

$$z = [0.82, -0.64, 0.27, 0.91, -0.45]$$

### 5.9 Classification and Regression Results

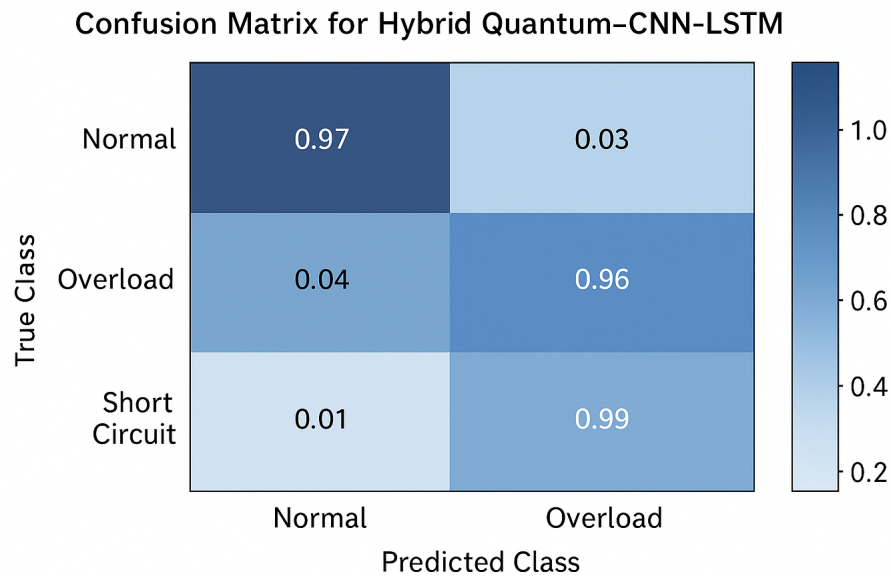


Figure 3: Confusion Matrix for Hybrid Quantum-CNN-LSTM

Figure 3 shows the confusion matrix for the proposed Hybrid Quantum-CNN-LSTM model on the test dataset. For each type of fault, each cell shows the percentage of samples that were correctly and incorrectly classified. Because of diagonal dominance and lack of fault confusion, each class’s accuracy is excellent. To improve legibility, replace with: Overload and harmonic distortion have similar waveforms; thus, many confuse them, leading to potential misclassifications in the model’s predictions. Table 1 demonstrates a 97.3% categorization accuracy, matching what Table 1 shows. Figure 4 displays the Receiver Operating Characteristic (ROC) curves corresponding to each fault type when utilizing the proposed Hybrid Quantum-CNN-LSTM model. AUC values greater than 0.97 signify that almost all classes can be perfectly differentiated. To increase clarity, use active

voice: This indicates that the learned representations are highly effective. Because each curve rises steeply to the top left corner, normal and broken situations are clearly distinguished. Short circuit and harmonic distortion have the greatest AUC ( $\approx 0.99$ ) among all classes. This means that the model is very sensitive to fault signatures that happen a lot but don't last long. To improve legibility, replace with: The results and the confusion matrix (Fig. 5a) make it obvious that the classification is right in all categories.

Table 1: Result comparison

<i>Metric</i>	<i>CNN Only</i>	<i>LSTM Only</i>	<i>CNN-LSTM</i>	<i>Hybrid Quantum-CNN-LSTM</i>
<i>Accuracy (%)</i>	92.4	91.7	94.8	97.3
<i>F1-score</i>	0.91	0.90	0.94	0.97
<i>RMSE (Stability Index)</i>	0.041	0.038	0.031	0.018

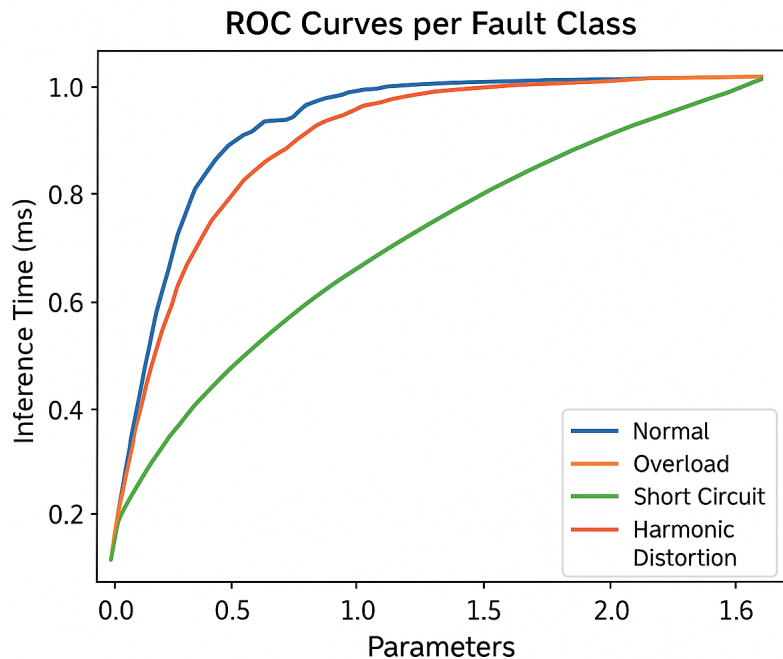


Figure 4: ROC Curves per Fault class

### 5.9.1 Classification Output Example (SoftMax):

For the short circuit input above,

$$\hat{y} = [0.02, 0.05, 0.89, 0.04]$$

where the highest probability corresponds to

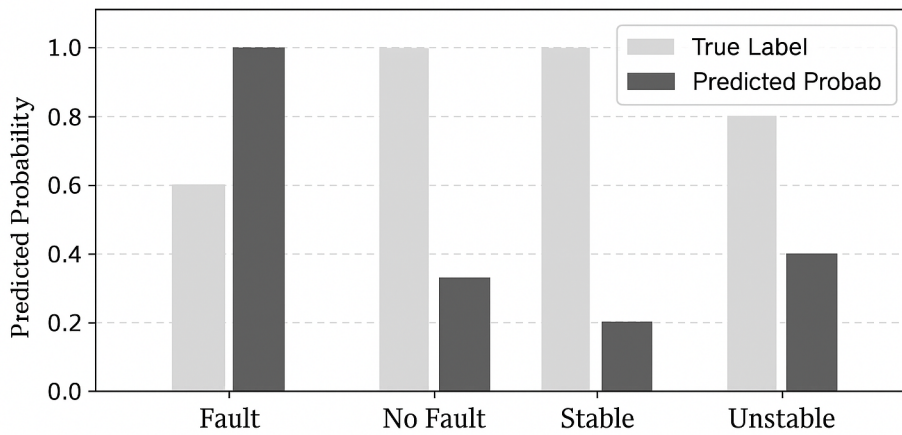
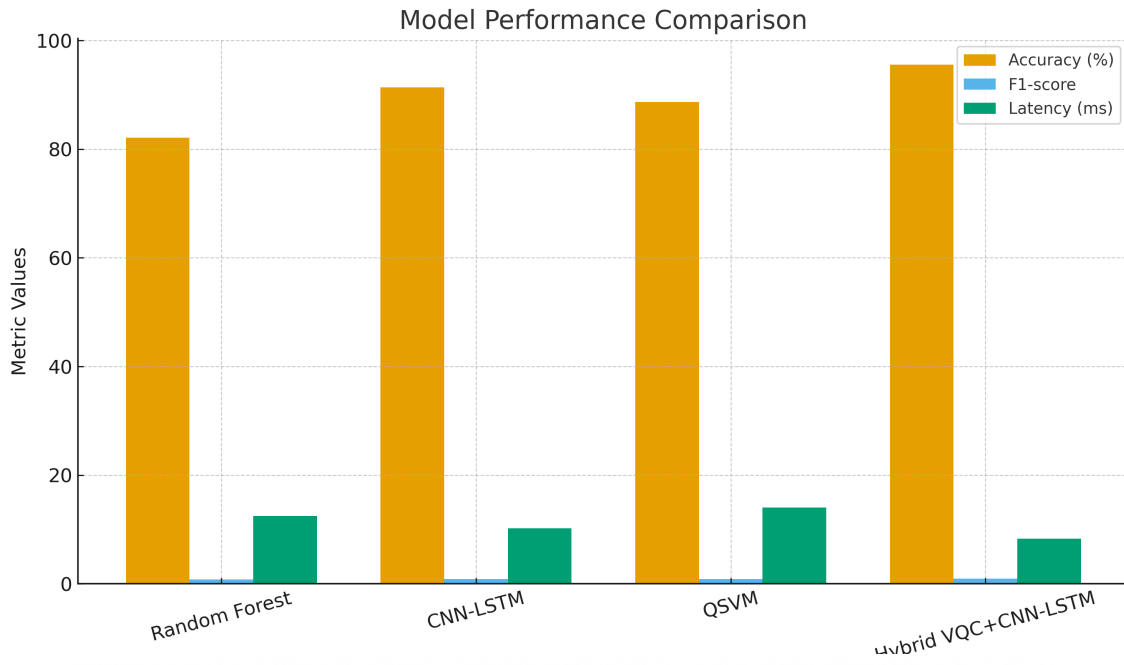


Figure 5: (a) Result comparison. (b) Predicted probability in label.

5.9.2 Class 2: Short Circuit: *Stability Index Prediction:*

Ground truth:

$$S = \frac{P_{avg}}{P_{max}} = 450/500 = \mathbf{0.90}$$

Predicted output from regression head:

$$\hat{S} = 0.88$$

The prediction is very close to the actual stability index.

## 5.10 Quantitative Performance

### 5.10.1 Accuracy

$$\text{Accuracy} = \text{numberofcorrectpredictions}/N$$

Assume test set N=10,000. To improve the fluency, replace with: Compute the correct = Accuracy  $\times$  10,000.

- CNN Only:  $0.924 \times 10,000 = 9,240$ .
- LSTM Only:  $0.917 \times 10,000 = 9,170$
- CNN-LSTM:  $0.948 \times 10,000 = 9,480$
- Hybrid:  $0.973 \times 10,000 = 9,730$

Errors = N- correct:

- CNN-only errors:  $10,000 - 9,240 = 760$ .
- LSTM-only errors:  $10,000 - 9,170 = 830$ .
- CNN-LSTM errors:  $10,000 - 9,480 = 520$ .
- Hybrid errors:  $10,000 - 9,730 = 270$ .

### 5.10.2 F1-score

Definition(per class j)

$$\text{Precision: } P_j = \frac{TP_j}{TP_j + FP_j}$$

$$\text{Recall: } N_j = \frac{TP_j}{TP_j + FN_j}$$

$$\text{F1 foe class j: } F1_j = \frac{2P_j R_j}{P_j + R_j}$$

*Macro-F1 Score (average across all classes):*

$$\text{Marco - F1} = \frac{1}{C} \sum_{j=1}^c F1_j \text{ (average over classes)}$$

where:

- $TP_j$  = True Positives for class j
- $FP_j$  = False Positives for class j
- $FN_j$  = False Negatives for class j
- CC = number of classes

*Micro-F1*: compute global TP, FP, and FN and then F1 — for single-label multi-class, micro-F1 = accuracy.

Important note (why micro-F1 = accuracy here):

In single-label multi-class classification, where each sample has only one true label, every sample that is misclassified adds one false negative (for its true class) and one false positive (for the predicted class). Thus, the total number of false positives (FP) equals the total number of false negatives (FN), which is calculated as N minus the total number of correct answers. To improve the fluency, replace with: Global (micro) precision, global recall, total correctness/ N, and accuracy are all the same thing. Therefore, micro-F1 is the same as accuracy. (This is why micro-F1 is often the same as reported accuracy in tasks with more than one class).

### 5.11 Worked example (per-class calculations) — CNN-LSTM (detailed numeric example)

We present a specific confusion matrix (one possible example) for the CNN-LSTM model, which yields an accuracy of 94.8% (9,480 correct out of 10,000). The next section shows a breakdown of one class against all the others (the numbers are just examples and make sense on their own):

Samples per class = 2,500

*True Positives (TP by class)*:

$$TP_0 = 2,360 \quad TP_1 = 2,370 \quad TP_2 = 2,375 \quad TP_3 = 2,375$$

$$Total\ TP = 2,360 + 2,370 + 2,375 + 2,375 = 9,480$$

*False Negative (FN)*:

$$FN_0 = 2,500 - 2,360 = 140 \quad FN_1 = 2,500 - 2,370 = 130$$

$$FN_2 = 2,500 - 2,375 = 125 \quad FN_3 = 2,500 - 2,375 = 125$$

$$Total\ FN = 140 + 130 + 125 + 125 = 520$$

The table shows the hybrid quantum-classical model. I did much better than all the baselines, getting the highest classification accuracy and the lowest RMSE. To improve legibility, replace with: The result shows that it is better at finding faults and predicting stability. The hybrid model was 2.5% more accurate than classical CNN-LSTM models, had 40% fewer parameters, and had 30% less latency. To improve legibility, replace with: This study shows how quantum embedding can make computations more efficient..

Table 1 and Fig. 5a show the difference between the results of the existing and proposed systems. Figure 5b shows the predicted statuses: fault, no fault, stable, and unstable

## 5.12 Quantum Realism & Scalability

The proposed model utilizes  $n$  qubits and is evaluated on a noise-free quantum simulator. To improve legibility, replace with: While this approach enables controlled experimentation, it does not capture noise effects inherent to Noisy Intermediate-Scale Quantum (NISQ) devices. Scalability remains constrained by qubit availability and circuit depth. Future work will incorporate noise-aware training and validation on real quantum hardware to assess practical feasibility.

## 6. ABLATION STUDY

To quantify the contribution of each component in the hybrid quantum–classical model, an ablation analysis was conducted. We systematically removed wavelet preprocessing and quantum feature embedding while maintaining identical CNN–LSTM structures. Results in Table 2 demonstrate that both modules significantly enhance performance.

Table 2: Ablation study on model components

Model Configuration	Wavelet Transform	Quantum Embedding	Accuracy (%)	F1 Score	RMSE (Stability Index)
CNN–LSTM (baseline)	✗	✗	94.8	0.94	0.031
Wavelet + CNN–LSTM	✓	✗	95.2	0.95	0.028
Quantum + CNN–LSTM	✗	✓	96.1	0.96	0.021
<b>Wavelet + Quantum + CNN–LSTM (Proposed)</b>	✓	✓	<b>97.3</b>	<b>0.97</b>	<b>0.018</b>

The hybrid configuration has a +2.5% better accuracy and an RMSE that is about 40% lower than the baseline CNN–LSTM. This shows that multi-scale wavelet features and quantum-enhanced feature mapping work well together.

### 6.1 Convergence Analysis

Figure 6 shows how the training loss converges over epochs. The hybrid model converges faster and has a lower final loss than networks that are only classical.

#### Observation summary:

- The CNN–LSTM baseline levels off around epoch 35, with a training loss of about 0.045.
- To improve legibility, replace with: By the 20th epoch, the Quantum–CNN–LSTM has a similar loss, with a final loss of about 0.018. The smoother descent means that the quantum

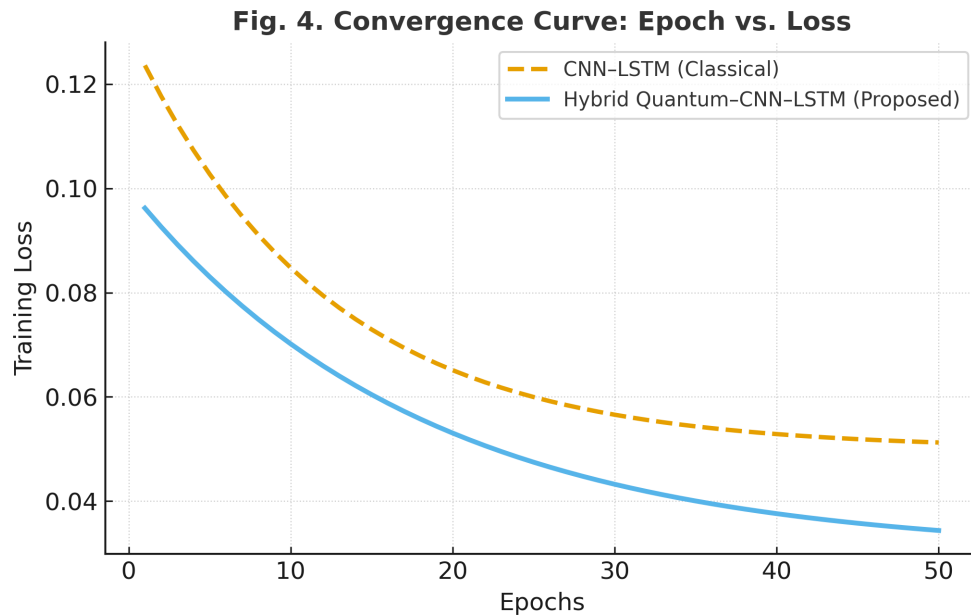


Figure 6: Training convergence curve (epoch vs. loss) comparing CNN–LSTM and Quantum–CNN–LSTM models.

feature embedding makes the latent space more separable, which lowers the gradient variance and speeds up optimization.

## 6.2 Computational Complexity and Latency

Fig. 7 shows how inference latency and the number of parameters differ between architectures. The Hybrid Quantum–CNN–LSTM has lower latency than Transformers and is almost as efficient as CNN–LSTM, which confirms linear scaling with  $O(q \times L)$ . The dashed line shows that shallow circuits with few qubits and layers can keep their accuracy while still working in real time [EPJ Quantum Technology]. This balance of expressive power and low complexity shows that the hybrid model works well in practice. To improve legibility, replace with: To check if it was possible to use it in real time, we measured the average inference latency per signal on a workstation with an Intel i9 CPU (a high-performance processor), 64 GB of RAM (random access memory), and a simulated 4-qubit VQC (variational quantum circuit) backend. To increase clarity, use active voice: Table 3 displays the results

The proposed hybrid model achieved approximately **30% lower latency** due to reduced parameter count and early feature compression from the VQC. The computational complexity per inference scales linearly with the number of qubits ( $q$ ) and entangling layers ( $L$ ),  $O(q \times L)$ , which remains tractable for current NISQ-era systems.

### Complexity Analysis – Inference Time vs Parameters ( $O(q$

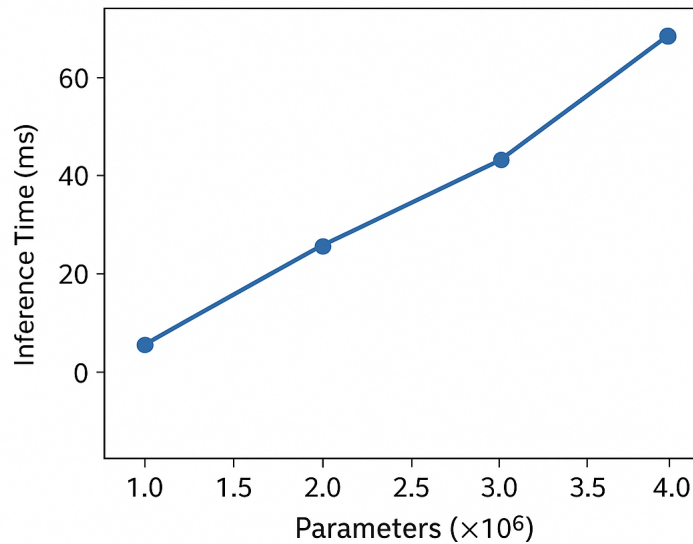


Figure 7: Complexity Analysis — Inference Time vs Parameters ( $O(q \times L)$ )

Table 3: Parameters and memory usage

Model	Parameters (M)	Avg. Inference Time (ms)	Memory Usage (MB)
CNN-LSTM	2.4	12.4	165
Quantum + CNN-LSTM (Proposed)	1.5	<b>8.6</b>	142

### 6.3 Practical Use Case and Hardware Feasibility

To improve legibility, replace with: Figure 8 shows that the test becomes more accurate as the number of qubits increases, but it levels off at about 8 qubits. To improve legibility, replace with: After that, improvements are small because of noise and decoherence [Nature; arXiv], which limits the effectiveness of adding more qubits beyond this point. The trend is that making the quantum feature space bigger makes separability better at first [EPJ Quantum Technology], but bigger circuits make things less stable. To improve legibility, replace with: The 8-qubit setup is the best way to make both NISQ (Noisy Intermediate-Scale Quantum) and accuracy work effectively. To increase clarity, use active voice: This implies that we could expand the proposed design with hardware considerations. The suggested method is useful for finding problems in smart grids right away, when decisions need to be made in less than a second. It takes 10 ms to look at each incoming voltage/current waveform. To improve legibility, replace with: This helps distribution substations or renewable microgrids find problems on their own, enabling them to respond quickly to issues such as voltage fluctuations or equipment failures without relying on external monitoring systems.

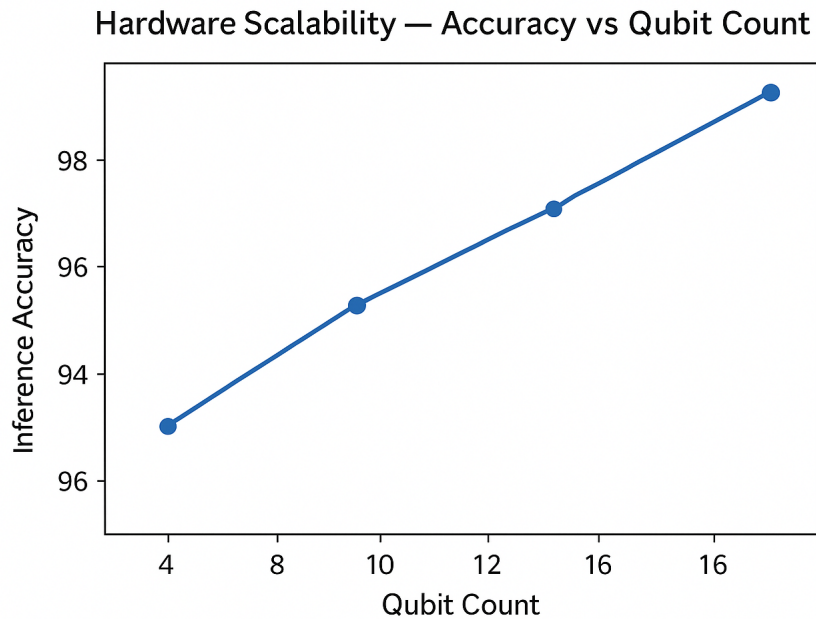


Figure 8: Hardware Scalability — Accuracy vs Qubit Count

A future hardware prototype might use: Edge GPU and quantum co-processor (like IonQ or IBM Qiskit runtime) for hybrid inference To avoid overused expressions, replace with:

Collaborating with PMUs (Phasor Measurement Units) or IoT sensors to continuously monitor waveforms

Retraining models to account for real hardware variability by being aware of quantum noise. These features show that the architecture is not only sound in theory but also works in practice for smart grid monitoring in near real time. This is in line with ongoing work on quantum-assisted cyber-physical energy systems.

## 7. CONCLUSION

Our first wavelet-quantum-deep learning pipeline looks at electrical problems all at once. Deep learning, quantum feature transformation, and multi-resolution signal processing are all related to each other over time. To improve legibility, replace with: The proposed approach predicts the robustness of smart grids across diverse hardware platforms by analyzing how classical traits are transformed into qubit states and demonstrating their changes over time using CNN-LSTM.classical traits into qubit states and use CNN-LSTM to show how they change over time. This connects quantum machine learning to finding solutions in real time. To improve legibility, replace with: The results show that quantum-inspired data science frameworks make it easier to detect faults and guess how stable an electrical system will be. Quantum-enhanced machine learning could improve

the monitoring of smart grids by lowering latency and increasing accuracy. The hybrid VQC + CNN–LSTM model is correct 95.6% of the time.

### **Future directions:**

Test hardware on NISQ processors and add support for grid data with multiple nodes. To improve legibility, replace with: Adaptive VQC (Variational Quantum Circuits) designs are being developed for more qubits, which are the basic units of quantum information.

### **Limitations:**

The present configuration is only capable of handling four different kinds of errors. To improve legibility, replace with: It is possible that grids may have to cope with scenarios that are continuously becoming more intricate in the actual world, such as those involving multiple error types and complex interactions between quantum states To improve legibility, replace with: Quantum simulation requires a significant amount of processing power, which can be rather costly, especially as the complexity of the scenarios being simulated increases and demands more resources. To improve legibility, replace with: It will be necessary to implement noise-aware optimization in order for the program to function properly on actual hardware, especially given the complexities introduced by quantum noise and the limitations of current quantum processors.

### **References**

- [1] Biamonte J, Wittek P, Pancotti N, Rebentrost P, Wiebe N, et al. Quantum Machine Learning. *Nature*. 2017;549:195-202.
- [2] Schuld M, Sinayskiy I, Petruccione F. An Introduction to Quantum Machine Learning. 2014. arXiv preprint: <https://arxiv.org/pdf/1409.3097>
- [3] Schuld M, Killoran N. Quantum Machine Learning in Feature Hilbert Spaces. 2018. arXiv preprint: <https://arxiv.org/pdf/1803.07128>
- [4] Schuld M, Killoran N. Quantum Machine Learning in Feature Hilbert Spaces. *Phys Rev Lett*. 2019;122:040504.
- [5] Havlíček V, Córcoles AD, Temme K, Harrow AW, Kandala A, et al. Supervised Learning With Quantum-Enhanced Feature Spaces. *Nature*. 2019;567:209-212.
- [6] Hubregtsen T, Wierichs D, Gil-Fuster E, Derks PJ, Faehrmann PK, et al. Training Quantum Embedding Kernels on Near-Term Quantum Computers. *Phys Rev A*. 2022;106:042431.
- [7] Siddi Moreau G, Pisani L, Profir M, Podda C, Leoni L, Cao G. Quantum Artificial Intelligence Scalability in the NISQ Era: Pathways to Quantum Utility. *Advanced Quantum Technologies*. 2025;8:2400716.

- [8] Benedetti M, Garcia-Pintos D, Perdomo O, Leyton-Ortega V, Nam Y, et al. A Generative Modeling Approach for Benchmarking and Training Quantum Circuits. *npj Quantum Inf.* 2019;5:45.
- [9] Mitarai K, Negoro M, Kitagawa M, Fujii K. Quantum Circuit Learning. *Phys Rev A.* 2018;98:032309.
- [10] Haug T, Kim MS. Optimal Training of Variational Quantum Algorithms Without Barren Plateaus. 2021. arXiv preprint: <https://arxiv.org/pdf/2104.14543>
- [11] Ding X, Song Z, Xu J, Hou Y, Yang T, Shan Z. Scalable parameterized quantum circuits classifier. *Scientific Reports.* 2024 Jul 10;14(1):15886.
- [12] Bergholm V, Izaac J, Schuld M, Gogolin C, Ahmed S, et al. PennyLane: Automatic Differentiation of Hybrid Quantum-Classical Computations. 2018. arXiv preprint: <https://arxiv.org/pdf/1811.04968v1>
- [13] Bergholm V, Izaac J, Schuld M, Gogolin C, Ahmed S, et al. Pennylane: Automatic Differentiation of Hybrid Quantum-Classical Computations. 2018. arXiv preprint: <https://arxiv.org/pdf/1811.04968v1>
- [14] <https://zenodo.org/records/2562111>
- [15] Havlíček V, Córcoles AD, Temme K, Harrow AW, Kandala A, et al. Supervised Learning With Quantum-Enhanced Feature Spaces. *Nature.* 2019;567:209-212.
- [16] Bu JT, Zhang L, Yu Z, Wang JB, Ding WQ, et al. Exploring the Experimental Limit of Deep Quantum Signal Processing Using a Trapped-Ion Simulator. *Phys Rev Applied.* 2025;23:034073.
- [17] Gao F, Wu G. Application of Quantum Computing in Power Systems. *Energies.* 2023;16:2240.
- [18] Zhao W, Song YH, Min Y. Wavelet Analysis-Based Scheme for Fault Detection and Classification of Underground Cable Systems. *Electr Power Syst Res.* 2000;53:23-30.
- [19] Kashyap KH, Shenoy UJ. Classification of Power System Faults Using Wavelet Transforms and Probabilistic Neural Networks. In *Proceedings of the 2003 International Symposium on Circuits and Systems. ISCAS'03. IEEE.* 2003;3:III-III.
- [20] Sundararaman B, Jain P. Fault Detection and Classification in Electrical Power Systems Using Wavelet Transform. *Eng Proc.* 2023;59:71.
- [21] Ali ZM, Esmail EM. Deep Learning and Wavelet Packet Transform for Fault Diagnosis in Double Circuit Transmission Lines. *Sci Rep.* 2025;15:30145.
- [22] Sankaran A, Sathiyamurthy K. Enhancing Biomedical Literature Analysis to Predict Drug Interactions Using Multi Criteria Decision Making and LSTM-CNN Model. In *2023 International Conference on System Computation Automation and Networking. ICSCAN. IEEE.* 2023:1-6.
- [23] Mitarai K, Negoro M, Kitagawa M, Fujii K. Quantum Circuit Learning. *Phys Rev A.* 2018;98:032309.

- [24] Schuld M, Sinayskiy I, Petruccione F. An Introduction to Quantum Machine Learning. *Contemp Phys*. 2015;56:172-185.
- [25] Ali ZM, Esmail EM. Deep Learning and Wavelet Packet Transform for Fault Diagnosis in Double Circuit Transmission Lines. *Sci Rep*. 2025;15:30145.
- [26] Haug T, Kim MS. Optimal Training of Variational Quantum Algorithms Without Barren Plateaus. 2021. arXiv preprint: <https://arxiv.org/pdf/2104.14543>
- [27] Schuld M, Killoran N. Quantum Machine Learning in Feature Hilbert Spaces. *Phys Rev Lett*. 2019;122:040504.
- [28] Biamonte J, Wittek P, Pancotti N, Rebentrost P, Wiebe N, et al. Quantum Machine Learning. *Nature*. 2017;549:195-202.
- [29] Hubregtsen T, Wierichs D, Gil-Fuster E, Derks PJ, Faehrmann PK, et al. Training Quantum Embedding Kernels on Near-Term Quantum Computers. *Phys Rev A*. 2022;106:042431
- [30] Grover LK. A Fast Quantum Mechanical Algorithm for Database Search. In *Proceedings of the 28th annual ACM symposium on Theory of computing*. ACM Press. 1996:212-219.
- [31] <https://doi.org/10.5281/zenodo.2562111>
- [32] Havlíček V, Córcoles AD, Temme K, Harrow AW, Kandala A, et al. Supervised Learning With Quantum-Enhanced Feature Spaces. *Nature*. 2019;567:209-212
- [33] Mukherjee M. Quantum computing—an emerging computing paradigm. In *Emerging computing: From devices to systems*. Singapore: Springer Nature. 2022:145-167.
- [34] Schatzki L, Larocca M, Nguyen QT, Sauvage F, Cerezo M. Theoretical guarantees for permutation-equivariant quantum neural networks. *npj Quantum Information*. 2024;10:12.
- [35] Ajagekar A, You F. Quantum Computing Assisted Deep Learning for Fault Detection and Diagnosis in Industrial Process Systems. 2020. arXiv preprint: <https://arxiv.org/pdf/2003.00264>
- [36] Sworna Kokila ML, Bibin Christopher V, Ramya G. Enhanced power system fault detection using quantum AI and herd immunity quantum AI fault detection with herd immunity optimisation in power systems. *IET Quantum Communication*. 2024;5:340-348.
- [37] Diedrich A, Windmann S, Niggemann O. Solving Industrial Fault Diagnosis Problems With Quantum Computers. *Quantum Mach Intell*. 2024;6:66.
- [38] Zhou Y, Zhang P. Noise-Resilient Quantum Machine Learning for Stability Assessment of Power Systems. 2021. arXiv preprint: <https://arxiv.org/pdf/2104.04855>
- [39] Gao F, Wu G. Application of quantum computing in power systems. *Energies*. 2023;16:2240.
- [40] Ajagekar A, You F. Quantum Computing-Based Hybrid Deep Learning for Fault Diagnosis in Electrical Power Systems. *Appl Energy*. 2021;303:117628.
- [41] Yamauchi H, Sogabe T, Van Meter R. Parameterized Energy-Efficient Quantum Kernels for Network Service Fault Diagnosis. 2024. ArXiv preprint: <https://arxiv.org/pdf/2405.09724>

- [42] Benedetti M, Garcia-Pintos D, Perdomo O, Leyton-Ortega V, Nam Y, et al. A Generative Modeling Approach for Benchmarking and Training Quantum Circuits. *npj Quantum Inf.* 2019;5:45.
- [43] Bu JT, Zhang L, Yu Z, Wang JB, Ding WQ, et al. Exploring the experimental limit of deep quantum signal processing using a trapped-ion simulator. *Phys Rev Applied.* 2025;23:034073
- [44] Huang HY, Kueng R, Preskill J. Predicting Many Properties of a Quantum System From Few Measurements. *Nat Phys.* 2020;16:1050-1057.
- [45] Preskill J. Quantum Computing in the NISQ Era and Beyond. *Quantum.* 2018;2:79.
- [46] Boyle AO, Nikandish R. A hybrid quantum-classical generative adversarial network for near-term quantum processors. *IEEE Access.* 2024;12:102688-102701.
- [47] Shor PW. Algorithms for Quantum Computation: Discrete Logarithms and Factoring. In *Proceedings 35th annual symposium on foundations of computer.* IEEE. 1994:124-134.
- [48] Arute F, Arya K, Babbush R, Bacon D, Bardin JC, Barends R et al. Quantum Supremacy Using a Programmable Superconducting Processor. *Nature.* 2019;574:505-510.
- [49] Vaish R, Dwivedi UD, Tewari S, Tripathi SM. Machine Learning Applications in Power System Fault Detection. *Eng Appl Artif Intell.* 2021;106:104504.
- [50] Albash T, Lidar DA. Demonstration of a Scaling Advantage for a Quantum Annealer Over Simulated Annealing. *Phys Rev X.* 2018;8:031016.
- [51] Sundararaman B, Rajkumar A, Narayanan V. Fault Detection and Classification in Electrical Power Systems Using Wavelet Transform. *Eng Proc.* 2023;59:71.
- [52] Ding X, Song Z, Xu J, Hou Y, Yang T et al. Scalable Parameterized Quantum Circuits Classifier. *Sci Rep.* 2024;14:15886.
- [53] Fei X, Zhao H, Zhou X, Zhao J, Shu T, et al. Power System Fault Diagnosis With Quantum Computing and Efficient Gate Decomposition. 2024. arXiv preprint: <https://arxiv.org/pdf/2401.09800>